ACS APPLIED MATERIALS & INTERFACES

Research Article

www.acsami.org

Nuclease-Functionalized Poly(Styrene-*b*-isobutylene-*b*-styrene) Surface with Anti-Infection and Tissue Integration Bifunctions

Shuaishuai Yuan,[†,§] Jie Zhao,[‡] Shifang Luan,*[,†] Shunjie Yan,[†,§] Wanling Zheng,[†] and Jinghua Yin*[,†]

[†]State Key Laboratory of Polymer Physics and Chemistry, Changchun Institute of Applied Chemistry, Chinese Academy of Sciences, Changchun 130022, People's Republic of China

[‡]Department of Chemistry, Georgia Southern University, P.O. Box 8064, Statesboro, Georgia 30460, United States

[§]University of Chinese Academy of Sciences, Beijing 100049, People's Republic of China

Supporting Information

ABSTRACT: Hydrophobic thermoplastic elastomers, e.g., poly(styrene-*b*-isobutylene-*b*-styrene) (SIBS), have found various in vivo biomedical applications. It has long been recognized that biomaterials can be adversely affected by bacterial contamination and clinical infection. However, inhibiting bacterial colonization while simultaneously preserving or enhancing tissue-cell/material interactions is a great challenge. Herein, SIBS substrates were functionalized with nucleases under mild conditions, through polycarboxylate grafts as intermediate. It was demonstrated that the nuclease-modified SIBS could effectively prevent bacterial adhesion and biofilm formation. Cell adhesion assays confirmed that nuclease coatings generally had no negative effects on L929 cell adhesion, compared with the virgin SIBS reference. Therefore, the as-reported nuclease coating may present a promising approach to inhibit bacterial infection, while preserving tissue-cell integration on polymeric biomaterials.

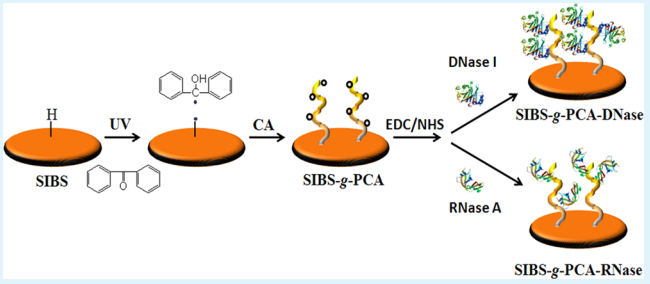

KEYWORDS: *poly(styrene-b-isobutylene-b-styrene) (SIBS), deoxyribonuclease (DNase), ribonuclease (RNase), antibacterial, cell adhesion*

INTRODUCTION

Thermoplastic elastomer (TPE), which possesses unique physical and biological properties, has gained great interest as a biomaterial over the past decades.[1] Styrenic TPE, particularly for poly(styrene-*b*-isobutylene-*b*-styrene) (SIBS), has been well used and explored in various in vitro and in vivo applications, such as catheters, drug-eluting stent coatings, heart leaflet valves, and ophthalmic implants,[2−5] because of its excellent oxidative, hydrolytic, and enzymatic stability over its lifespan in the body.

However, similar to most hydrophobic polymers, bacteria tend to adhere on the device surfaces made of SIBS, and form biofilms within which bacteria have increased resistance to antimicrobials and host immune system.[6,7] Therefore, suppression of bacterial attachment and biofilm formation has been of great interest to researchers.[8] For avoiding bacterial infection, one common approach is creating nonfouling surfaces that passively prevent the initial bacterial adhesion through the hydration of hydrophilic polymers, e.g., poly(ethylene glycol) (PEG),[9,10] poly(carboxybetaine methacrylate),[11−15] poly(sulfobetaine methacrylate),[16−21] poly(acrylamide)s,[22,23] neutral polysaccharides,[24] and poly(*N*-vinylpyrrolidone).[25] Another common approach is to actively kill bacteria relying on the incorporation of antibiotics,[26] or antimicrobials, such as silver ions,[27] N-halamine compounds,[28,29] cationic polymers,[30−35] and enzymes.[36,37]

Biomaterials, particularly for permanent implants, are required to possess good tissue integration performances. However, most surfaces tailored to prevent bacterial colonization do not effectively integrate with tissues.[38] Hence, constructing surfaces that prevent bacterial colonization while simultaneously promoting interactions with desirable mammalian cells, is an urgent task.[39] Surfaces with functionalities that reliably select mammalian cells over bacteria have been recently reported.[38−40] Kang et al. reported that a surface first modified with an antifouling coating, followed by immobilizing arginine-glycine-aspartic acid (RGD) peptide, can promote osteoblast functions and inhibit bacterial adhesion.[40]

Notably, nucleic acids, including deoxyribonucleic acid (DNA) and ribonucleic acid (RNA), as components of biofilm extracellular polymeric substances (EPS), have played essential roles in bacterial adhesion and biofilm formation.[41,42] In detail, extracellular DNA (eDNA) deriving from lysed bacteria can aid bacterial adhesion and maintain the structural integrity of biofilms.[43] The roles of RNA involved in biofilm development

Received: July 26, 2014
Accepted: September 25, 2014
Published: September 25, 2014

are unclear because of the relevant research field still in its infancy. They possibly act in core regulatory pathways of biofilm formation, such as those regulating motility and matrix production.[44] Since nucleic acids are critical in bacterial adhesion and biofilm formation, attacking and cleaving them by their specific nucleases, i.e., deoxyribonuclease (DNase) and ribonuclease (RNase) should be an effective antibacterial strategy. Whitchurch et al. first reported that DNase could nonspecifically cleave DNA by breaking the phosphodiester bonds of the phosphate backbone through hydrolysis, and in growth medium could inhibit biofilm formation and also rinsing a biofilm with DNase could effectively disintegrate 60 h old biofilms.[43] Similar effects of DNase on pretreating bacteria prior to their adhesion or post-treating biofilms have been successively reported.[45,46] The nuclease approaches to disrupt biofilms are based on nonbactericidal mechanisms, and thereby do not place a direct evolutionary pressure on the bacteria to develop resistance. In addition, they have nearly no adverse effects on the mammalian cells. Recently, Swartjes et al. investigated the antimicrobial efficacy of the covalently immobilized DNase coating in nature.[47]

In this work, the nuclease-functionalized SIBS samples were prepared under mild conditions through polycarboxylate grafts as intermediate. The biological performances of the DNase- and RNase-functionalized samples were comparatively evaluated by a series of experiments, e.g., in vitro response of L929 fibroblast and antibacterial efficacy.

EXPERIMENTAL SECTION

Materials. Poly(styrene-*b*-isobutylene-*b*-styrene) (SIBS) with 30 wt % PS hard blocks was kindly provided by Kaneka Americas. 2-Carboxyethyl acrylate (CA), deoxyribonuclease I (DNase I; isoelectric point (p*I* = 5.06)) and ribonuclease A (RNase A; p*I* = 9.6) were obtained from Sigma-Aldrich. Ribolock ribonuclease inhibitor was provided by Thermo Scientific. Benzophenone (BP) was supplied by Peking Ruichen Chemicals (China). 1-Ethyl-3-(3-(dimethylamino)-propyl) carbodiimide (EDC) hydrochloride and *N*-hydroxysuccinimide (NHS) were provided by Alfa Aesar. Phosphate buffered solution (PBS; 0.1 mol/L, pH = 7.4), 2-(*N*-Morpholino) ethanesulfonic acid (MES), Tween 20, sodium dodecyl sulfate (SDS), and bovine serum fibrinogen (BFg; p*I* = 5.6) were provided by Dingguo Biotechnology Co., Ltd. The Micro BCA protein assay reagent kit (AR1110) was purchased from Boster Biological Technology. Dulbecco's modified Eagle's medium (DMEM) and 0.25 wt % trypsin were purchased from Beijing Solarbio Science & Technology. Sterile filtered fetal bovine serum (FBS) was supplied by Beijing Yuanhengjinma Biotechnology. Fluorescein Isothiocyanate Labeled Phalloidin (FITC-Phalloidin) and 4′,6-diamidino-2-phenylindole (DAPI) dihydrochloride were provided by Sigma-Aldrich. Gram-negative *Escherichia coli* (*E. coli*; ATCC 25922) and Gram-postive *Staphylococcus aureus* (*S. aureus*; ATCC 6538), Luria−Bertani (LB) broth, and trypticase soy broth (TSB) were obtained from Dingguo Biotechnology Co., Ltd. The LIVE/DEAD Backlight Bacterial Viability Kit L7012 was purchased from Molecular Probe Inc., Eugene, OR. Other reagents were AR grade and all the materials were used as-received directly without further purification.

Surface Modification of SIBS Substrates. Photografting polymerization of CA on the SIBS substrates were conducted as follows. The substrates were ultrasonically cleaned in deionized water and ethanol for 5 min in each step. The clean substrates were immersed in the ethanol solution of BP photoinitiator (1 wt %) for about 20 min and dried at room temperature. Then the water solution of CA (10 wt %) was deposited onto the substrates and irradiated with UV light (high-pressure mercury lamp, 400 W, main wavelength 380 nm) to conduct the photografting polymerization of CA for the time ranging from 90 to 240 s. The SIBS substrates modified with poly(2-carboxyethyl acrylate) (SIBS-*g*-PCA) were washed with deionized water and ethanol to remove residual monomer, followed by drying in a vacuum oven. Grafting density (GD; $\mu g/cm^2$) of PCA was calculated as follows:

$$\mathrm{GD} = \frac{W_1 - W_0}{S}$$

where W_0 and W_1 are the weights (μg) of the virgin and modified substrates, respectively. S represents the surface area (cm^2) of the substrate. Each result is an average of at least three parallel experiments.

SIBS-*g*-PCA substrates (photografting time of 210 s) were then activated in 0.4 M EDC and 0.1 M NHS (MES solution) for 1 h. The activated substrates were immersed in DNase I or RNase A solution (1 mg/mL in PBS) for 12 h at room temperature under static conditions to prepare the nuclease-functionalized samples (denoted as SIBS-*g*-PCA-DNase or SIBS-*g*-PCA-RNase). The physically adsorbed nucleases were removed by ultrasonic processing with 0.5 wt % Tween 20 in PBS for 30 min. The substrates were then rinsed with sterile ultrapure water, stored at −20 °C and used within 14 h. According to the literatures,[47] SIBS-*g*-PCA-DNase and SIBS-*g*-PCA-RNase were inactivated through heating at 68 °C for 10 min and treating with 10U/μL RNase inhibitor at 37 °C for 12 h, respectively. The inactive DNase- and RNase-functionalized samples were used for determining the effect of enzymatic activity on preventing bacterial adhesion and biofilm formation.

Surface Characterization. ATR-FTIR spectra were obtained from a Fourier transform infrared spectrometer (FTIR; BRUKER Vertex 70). A total of 32 scans were accumulated with a resolution of 4 cm^{-1} for each spectrum. Surface elemental compositions were examined by an X-ray photoelectron spectroscopy (XPS; VG Scientific ESCA MK II Thermo Avantage V 3.20 analyzer) with Al/K ($h\nu$ = 1486.6 eV) anode mono-X-ray source at the detection angle of 90°. Scans between 1200 and 0 eV were performed and high-resolution spectra and their peak fitting curves were generated to monitor the formation of functional groups on the substrate. Water contact angle (WCA) was measured with a drop shape analysis instrument (DSA; KRÜSS GMBH, Germany) at room temperature. A 2 μL droplet of water was initially deposited onto the surface. The contact angle values were an average of five measurements on different areas of each sample.

Bacterial Adhesion and Biofilm Formation. *E. coli* and *S. aureus* were inoculated onto separated agar plates, and incubated overnight at 37 °C. A single colony of each bacterium from the agar plate was used to inoculate 10 mL of LB for *E. coli* and 10 mL of TSB for *S. aureus*, and cultured for 24 h at 37 °C. These cultures were in turn used to inoculate a 200 mL main culture in LB or TSB, which was grown for 24 h prior to harvesting. The bacteria containing growth broth were then centrifuged at 2700 rpm for 10 min to remove the supernatant. Bacterial cell concentration was calculated by testing the absorbance of cell dispersions at 540 nm relative to a standard calibration curve.[48] An optical density of 1.0 at 540 nm is equivalent to $\sim 10^9$ cells/mL. After removing the supernatant, the bacterial cells were diluted with PBS to 10^8 cells/mL. For initial adhesion, the samples were placed in 24-well plates and covered with bacterial suspension (2 mL) at 37 °C. Bacterial suspensions were removed after 60 min, and the substrates were gently washed with PBS. The efficacy of the nuclease-modified SIBS in inhibiting biofilm formation was assessed after incubation in growth medium containing 10^8 bacterial cells mL^{-1} for 10 h at 37 °C. Then growth medium was decanted and the biofilms were gently rinsed with PBS in order to remove planktonic bacteria. For assessing the viability of adherent bacteria on the various SIBS samples, the samples were stained by a combination dye (LIVE/DEAD Bac Light Bacterial Viability Kit) and observed under confocal laser scanning microscopy (CLSM; LSM 700, Carl Zeiss). The LIVE/DEAD BacLight Bacterial Viability assay utilize mixtures of SYTO 9 green fluorescent nucleic acid dye stain and red fluorescent nucleic acid dye propidium iodide (PI). As for this assay, viable (appearing green) and dead (appearing red) bacterial cells can be distinguished with fluorescent microscopy. The percentage of the occupied area of

Scheme 1. Photografting Polymerization of CA and the Subsequent Nuclease Immobilization

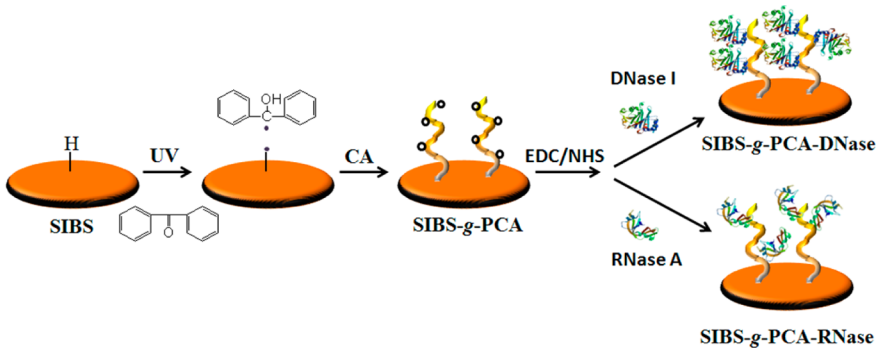

adhered bacteria from the fluorescent images were counted using ImageJ software.

Protein Adsorption. After soaking in PBS solution at room temperature for 12 h, the substrates were dipped into PBS solution containing BFg (1.0 mg/mL) at 37 °C for 2 h. Each substrate was sequentially rinsed five times with fresh PBS, immersed in an aqueous solution of 1.0 wt % SDS, and oscillated at 37 °C for 1 h to remove the adsorbed proteins from the substrate. On the basis of bicinchoninic acid (BCA) protein assay kit, the absorbance values of the SDS solution containing proteins was measured with a microplate reader (TECAN SUNRISE, Swiss), and amount of the adsorbed proteins was calculated. The reported data were the mean values of triplicate specimens for each substrate.

To determine the effect of protein on bacterial adhesion, *S. aureus* adhesion on the various SIBS substrates after pretreated with BFg (1.0 mg/mL) at 37 °C for 2 h was investigated using the procedure described above.

Cell Attachment Assay. Cell attachment assay was studied using murine fibroblasts cell line L929. Cells were grown in DMEM supplemented with 10 vol % FBS, 4.5 g/L Glucose, 100 units/mL penicillin, and 100 μg/mL streptomycin and maintained in a humidified 5 vol % CO_2/95 vol % air incubator at 37 °C. The cells were detached from the culture flask by addition of trypsin solution in PBS, and the cell suspension was transferred to a tube and centrifuged for 5 min. After removal of the trypsin, the remaining cells were resuspended in fresh medium for subsequent experiments. The viability of the cells was assayed by trypan blue exclusion method, and batches of cells with at least 95% viability were used for further experiments.

The substrates with diameter of 16 mm were placed in the wells of a 24-well culture plate. L929 fibroblast cells were seeded into the wells at a density of 1×10^5 cells/well and incubated at 37 °C under a 5 vol % CO_2 humidified atmosphere. After the L929 were cultured in the medium for 24 h, the substrates were carefully washed thrice with PBS, and then were fixed with 4 wt % paraformaldehyde at 37 °C for 30 min, followed by 5 min washing with PBS. Subsequently, cells were stained for 30 min with 1 mL PBS containing 10 μL DAPI and 5 μg/mL of FITC-phalloidin. The substrates were then washed 3 times in the PBS and examined with CLSM. To quantify cell adhesion, images were analyzed with ImageJ software to determine average cell density and total projected area. The density of cells was measured by counting the number of DAPI-stained nuclei from three different substrates. The total projected area was obtained by measuring the actin-stained cells.

Statistical Analysis. All data are presented as mean ± standard deviation (SD). The statistical significance was assessed by analysis of variance (ANOVA), * ($p < 0.05$), ** ($p < 0.01$), and *** ($p < 0.001$). Each result is an average of at least three parallel experiments.

RESULTS AND DISCUSSION

As illustrated in Scheme 1, the PCA-functionalized SIBS substrates were first prepared through photografting polymerization approach. This surface modifcation approach is chosen in our experiment, because it is particularly attractive for real-world applications.[49−52] Furthermore, the GD of photografting polymerization is commonly high, and can be effectively adjusted through graft parameters. In our experiment, when UV irradiated, benzophenone (BP) molecules are excited to undergo hydrogen-abstracting reactions from the SIBS macromolecular chains, consequently providing surface radicals ($R^{\bullet}$) capable of initiating surface graft polymerization of CA. As shown in Supporting Information (SI) Figure S1, the GD of PCA initially increased, and attained a maximum value of 50 μg/cm^2, as photografting time increased. Then EDC/NHS chemistry, which can covalently attach bioactive molecules such as enzymes and antibodies under mild conditions, was employed for the chemical immobilization of nuclease onto the SIBS-*g*-PCA substrate.[36,53]

Surface Characterization. Figure 1 presents the ATR-FTIR spectra of the samples. The graft polymerization of CA

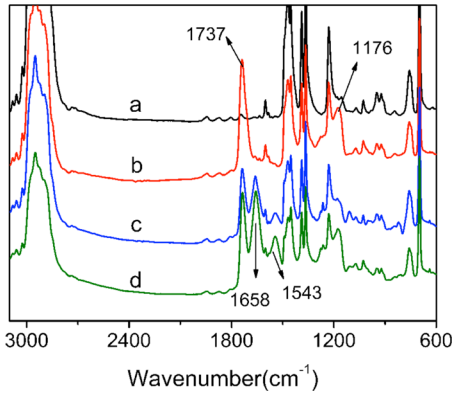

Figure 1. ATR-FTIR spectra of (a) virgin SIBS, (b) SIBS-*g*-PCA, (c) SIBS-*g*-PCA-DNase, and (d) SIBS-*g*-PCA-RNase.

onto the SIBS substrate was confirmed, since new peaks appeared at about 1737 cm^{-1} (C═O) and 1176 cm^{-1} (C—O). After the covalent attachment of nuclease, new peaks at 1658 cm^{-1} (amide I stretch vibrations, O═C—N) and 1543 cm^{-1} (amide II groups, N—H) were obviously observed.

The chemical compositions of the substrates at different surface modification stages were further examined by XPS. As shown in SI Figure S2, the strong N_{1s} peaks at 399.5 eV were detected on the nuclease-functionalized samples. As for SIBS-*g*-PCA-DNase and SIBS-*g*-PCA-RNase, their N/C values were about 11.7% and 7.6%, respectively (Table 1). As high-resolution C_{1s} XPS spectra and their peak fitting curves of the samples given in Figure 2, there was only one peak attributing

Table 1. Surface Compositions of the Various SIBS Samples

sample	composition (at.%) C	O	N	N/C (%)
SIBS	95.05	4.95		
SIBS-*g*-PCA	65.62	34.14	0.24	0.36
SIBS-*g*-PCA-DNase	70.27	21.48	8.25	11.74
SIBS-*g*-PCA-RNase	74.28	20.01	5.71	7.68

to the C—H/C—C species at 284.6 eV, as for the virgin SIBS (Figure 2(a)). After grafting with PCA brush, the C_{1s} spectrum could be curve-fitted into three peaks, i.e., C—H/C—C (at 284.6 eV), C—O (at 286.0 eV), and O—C═O (at 288.6 eV) species, respectively (Figure 2(b)). The C_{1s} curves of the nuclease-functionalized samples were generally decomposed into five peaks: C—H/C—C (at 284.6 eV), C—N (at 285.4 eV), C—O (at 285.9 eV), O═C—N (at 287.5 eV), and O═C—O (at 288.5 eV) species (Figure 2(c, d)).

Bacterial Adhesion and Biofilm Formation Evaluation. Construction of surface resistance to bacterial adhesion is an extremely important step to prevent bacterial-associated infection. Bacteria will rapidly colonize and form biofilms after the initial attachment. The bacteria in the biofilm demonstrate up to 1000 times higher resistance to host's natural defense systems as well as antibiotics, compared with planktonic ones.[54] Biofilms, in most cases, will lead to bacterial infections that are associated with indwelling biomaterials. Once a biofilm is established, replacement of the infected biomaterials would be the only choice. Therefore, development of an effective approach to resist bacterial adhesion and biofilm formation will offer important therapeutic benefits. The efficacy of the nuclease-modified SIBS substrates in inhibiting bacterial adhesion was assessed using the model bacteria. Figure 3 shows the CLSM images of adherent *E. coli* and *S. aureus* after 60 min incubation. Bacteria prefer to adhere on the hydrophobic surface through hydrophobic interaction,[55] therefore, a large number of bacteria were observed on the virgin SIBS after incubation in PBS (Figure 3(a)). The bacterial adhesion on the nuclease-functionalized samples was dramatically reduced (Figure 3(c),(d)).The initial bacteria coverage on SIBS-*g*-PCA-DNase was decreased by 94.8% for *E. coli* and 97.1% for *S. aureus* relative to the virgin SIBS reference (Figure 3(e),(f)). The bacterial coverage on SIBS-*g*-PCA-RNase had no statistically significant differences in comparison with SIBS-*g*-PCA-DNase. As shown in SI Figure S3, the *E. coli* coverage on the inactive DNase coating was about 10-fold higher than the active one. Thus, prevention of initial bacteria adhesion on SIBS-*g*-PCA-DNase could mainly be attributed to the enzymatic activity of the DNase moieties.[43,47] As reported by the previous researchers,[56,57] the antibacterial activity of RNase was not dependent on its enzymatic activity. In our experiments, we also observed that the loss of enzymatic activity of RNase had

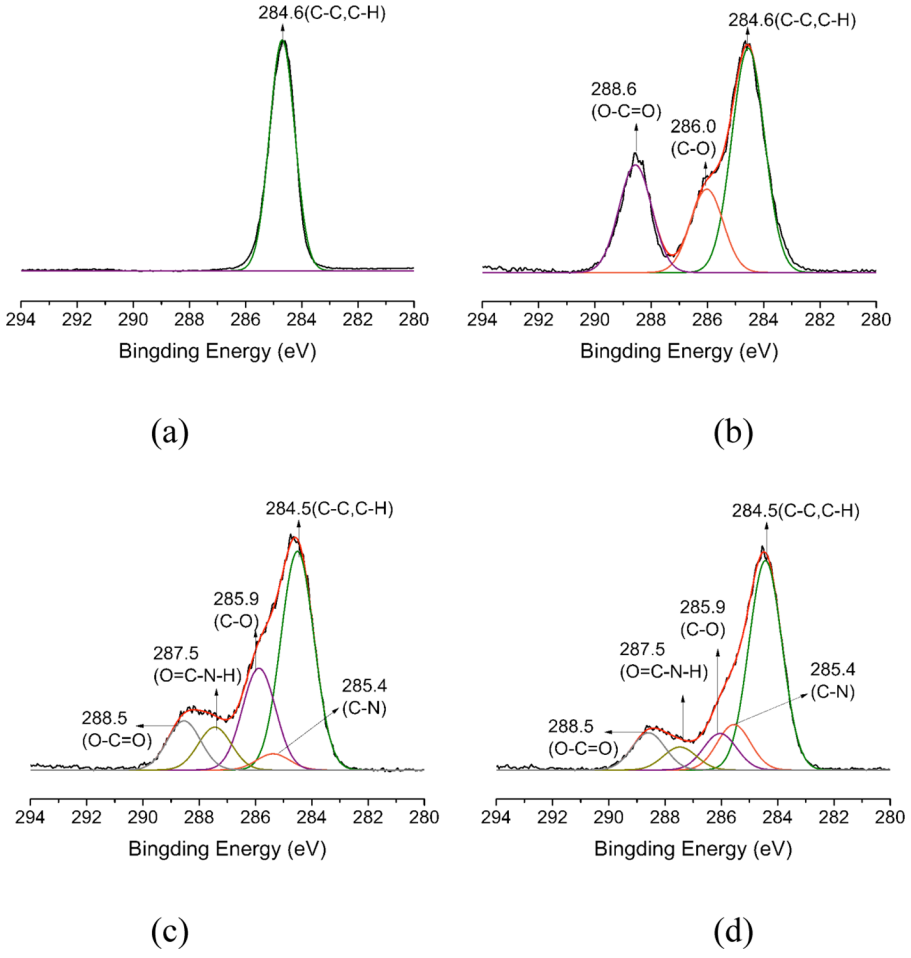

Figure 2. High-resolution C_{1s} XPS spectra and their peak fitting curves of the samples. (a) Virgin SIBS, (b) SIBS-*g*-PCA, (c) SIBS-*g*-PCA-DNase, and (d) SIBS-*g*-PCA-RNase.

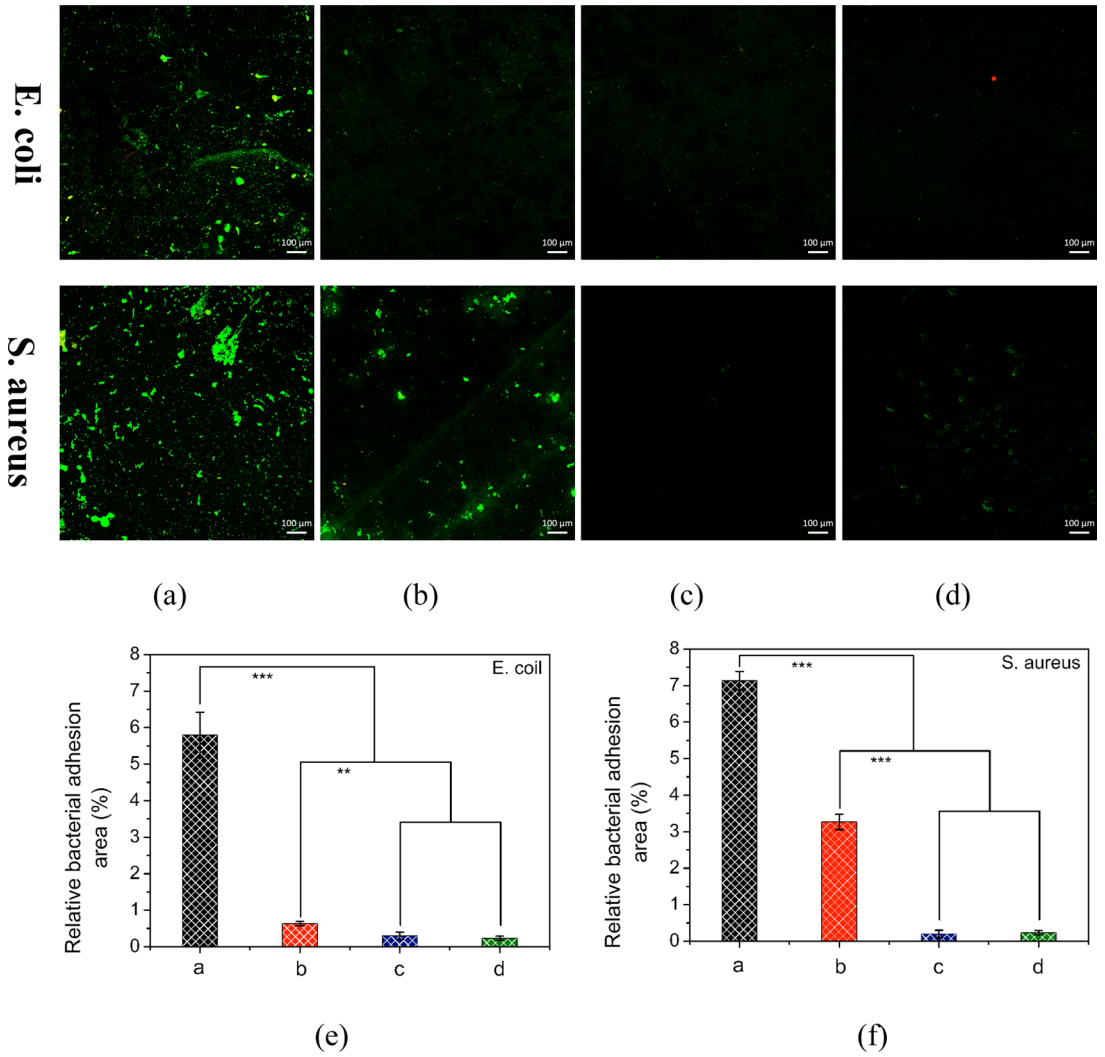

Figure 3. Representative CLSM images of *E. coli* and *S. aureus* adhesion on (a) virgin SIBS; (b) SIBS-*g*-PCA; (c) SIBS-*g*-PCA-DNase; and (d) SIBS-*g*-PCA-RNase samples after exposure to a PBS suspension of bacteria (10^8 cells mL^{-1}) for 60 min. Scale bar is 100 μm. Percentage of occupied area of adherent *E. coli* (e) and *S. aureus* (f) on various substrates after incubation in growth medium for 60 min. Significant difference (* $p < 0.05$; ** $p < 0.01$; and *** $P < 0.001$).

limited effect on the adhesion of *E. coli* (SI Figure S3(b),(e)). So the ability to inhibit bacterial adhesion of SIBS-*g*-PCA-RNase should be mainly associated with its high hydrophilicity (a WCA of ~18°) arising from the RNase moieties (SI Figure S4).

The initial stage after surgery has been identified as the period where prevention of biofilm formation is most critical to the long-term success of an implant.[58] Herein, the efficacy of the nuclease coatings in preventing biofilm formation was evaluated after incubation in growth medium for 10 h. It has been confirmed that eDNA could maintain the structural integrity of biofilms through specific and non-specific interaction with bacteria, so the removal or degradation of eDNA could effectively inhibit biofilm formation.[43] As shown in Figure 4, no obvious *E. coli* and *S. aureus* biofilms were observed on SIBS-*g*-PCA-DNase, while the bacteria readily formed biofilms on the virgin SIBS references. The bacterial coverage of *E. coli* and *S. aureus* was reduced from ~88.0% and ~68.1% of the virgin SIBS reference to ~0.3% and ~2.6% of SIBS-*g*-PCA-DNase, respectively. After the inactivation of DNase coating, its bacterial coverage of *E. coli* was greatly increased (SI Figure S3(c),(f)). Therefore, the enzymatic activity of DNase moieties was considered the major reason for inhibiting biofilm development. SIBS-*g*-PCA-RNase showed a much lower bacterial coverage, relative to the virgin SIBS reference. The bacterial coverages were reduced to ~1.5% for *E. coli*, while ~21.4% for *S. aureus*, which demonstrated that SIBS-*g*-PCA-RNase was more effective in preventing *E. coli* biofilm than *S. aureus* biofilm. Identification of the antimicrobial mechanisms of RNase was very important, which would contribute to the understanding of the proteins involved in the innate immunity.[59] Although the related investigation is very difficult, it should be clarified through the wide collaboration of researchers as soon as possible.

Effect of Protein Adsorption on Bacterial Adhesion. Numerous factors promote bacterial adhesion to the surface, such as physico-chemical interactions and bacterial surface biochemical components. Among molecular determinations promoting bacterial adhesion, proteins are the most functionally diverse active components. In this work, BFg adsorption on the various substrates was investigated. The amount of BFg adsorbed on the virgin SIBS was ~6.5 μg cm^{-2}. After grafting with PCA, it was greatly reduced to ~2.8 μg cm^{-2}. After the immobilization of nuclease, it was further decreased (Figure 5).

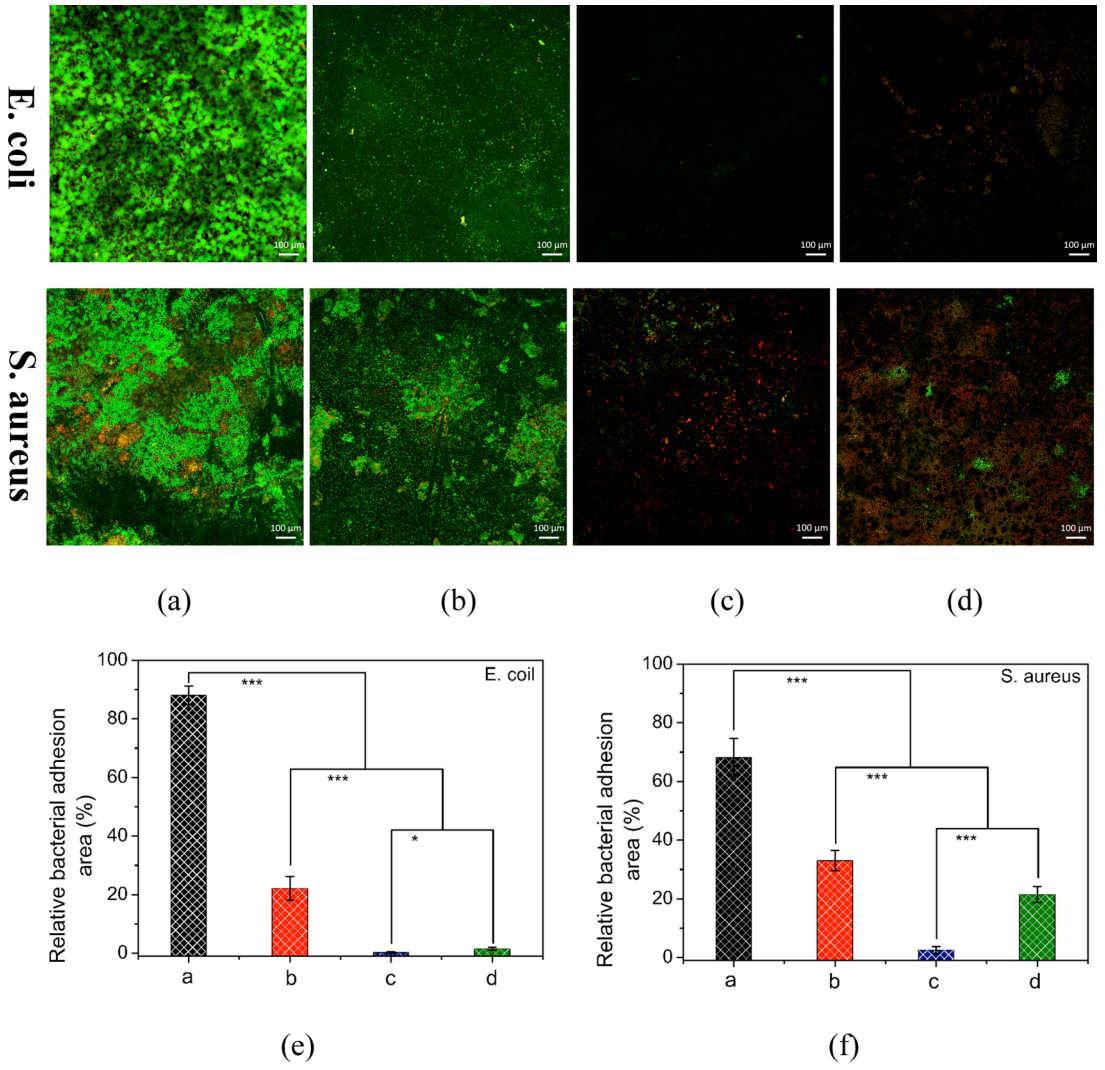

Figure 4. Representative CLSM images of *E. coli* and *S. aureus* on (a) virgin SIBS; (b) SIBS-*g*-PCA; (c) SIBS-*g*-PCA-DNase; (d) SIBS-*g*-PCA-RNase surfaces; (e) Relative bacterial adhesion area of *E. coli*; and (f) Relative bacterial adhesion area of *S. aureus* after incubation in growth medium containing 10^8 bacterial cells mL^{-1} for 10 h. Scale bar is 100 μm. Significant difference (* $p < 0.05$; ** $p < 0.01$; and *** $P < 0.001$).

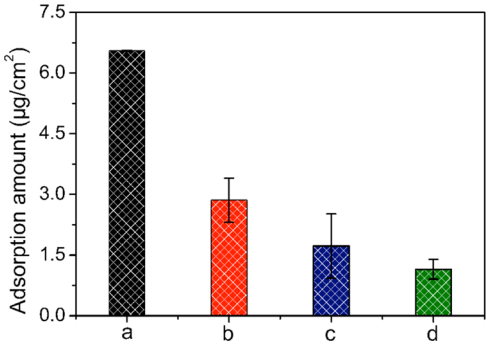

Figure 5. BFg protein adsorption on (a) virgin SIBS, (b) SIBS-*g*-PCA, (c) SIBS-*g*-PCA-DNase, and (d) SIBS-*g*-PCA-RNase.

The observed reduction in protein adsorption on SIBS-*g*-PCA-DNase can be correlated with its hydrophilicity and negatively charged property. As for SIBS-*g*-PCA-RNase, its hydrophilicity is mainly responsible for protein resistance.

BFg and *S. aureus* were used to investigate the effect of protein adsorption on subsequent bacterial adhesion. SI Figures S5 and S6, respectively, present the representative CLSM images and percentages of adherent *S. aureus* on the substrates after preadsorbing with BFg solution. After pretreatment with BFg solution, the bacterial coverages on the virgin SIBS reference and SIBS-*g*-PCA were greatly increased, that was consistent with the results reported previously.[60] This phenomenon was attributed to the BFg binding protein expressed by *S. aureus*.[61] In contrast, the bacterial coverage on the nuclease-functionalized samples had nearly no change before and after pretreatment with BFg solution because of the good antifouling properties of nucleases.

Cell Adhesion. A surface tailored to possess antibacterial performance usually has adverse effects on the interaction with cells. Herein, the adhesion and proliferation of L929 cells on the nuclease-functionalized substrates were investigated. A large number of L929 cells were readily attached, spread, and mostly covered with round-shaped cells (Figure 6(a)). In contrast, the L929 cells were barely adhered and spread on SIBS-*g*-PCA (Figure 6(b)). The cell density and total projected area of SIBS-*g*-PCA were statistically significantly lower than that of the virgin SIBS references (Figure 7(A),(B)). Compared to the virgin SIBS, the cell density and total projected area of SIBS-*g*-PCA-DNase had no obvious change. These findings correlate

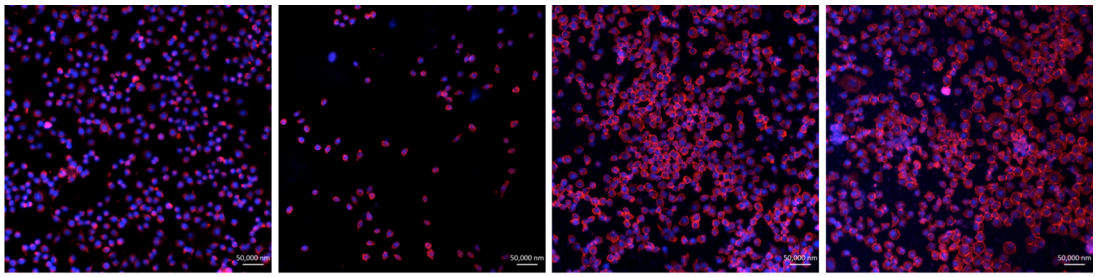

Figure 6. Representative CLSM images of L929 fibroblast cells on the supports for 24 h incubation and stained for nuclei (blue), actin (red). (a) Virgin SIBS, (b) SIBS-*g*-PCA, (c) SIBS-*g*-PCA-DNase, and (d) SIBS-*g*-PCA-RNase surfaces. Size of the scale bars: 50 μm.

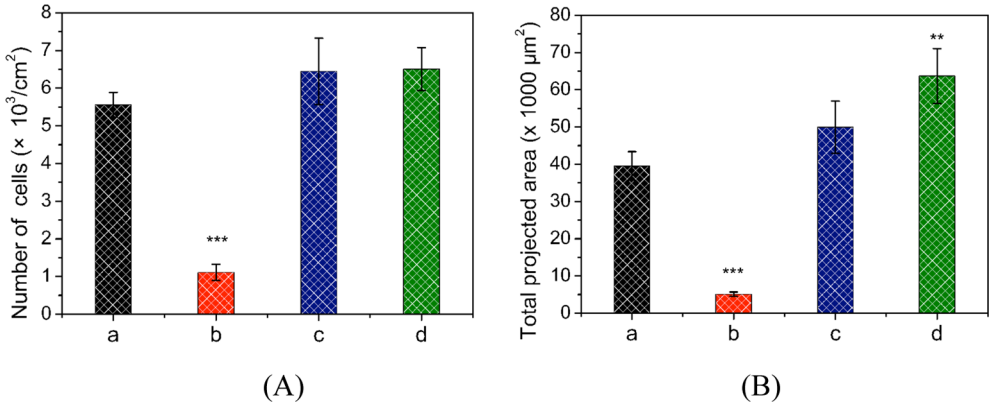

Figure 7. Statistical analysis of (A) adherent L929 fibroblast cells density, and (B) quantification of total projected area on (a) virgin SIBS; (b) SIBS-*g*-PCA; (c) SIBS-*g*-PCA-DNase; and (d) SIBS-*g*-PCA-RNase surfaces. Significant difference (** $p < 0.01$ and *** $p < 0.001$) compared with the virgin SIBS.

with the results of the earlier work that the DNase coating had no negative effect on the cell adhesion and proliferation.[47] The total projected area of SIBS-*g*-PCA-RNase was statistically significantly larger than that of the virgin SIBS reference.

CONCLUSIONS

In this work, a novel strategy for preventing bacterial adhesion and biofilm formation by nuclease coating has been proposed. Surface characterization confirmed the successful immobilization of nucleases onto SIBS substrates. The nuclease-modified SIBS presented good antiadhesion and antibiofilm properties against *E. coli* and *S. aureus*. The enzymatic activity of DNase could play an important role in inhibiting bacterial infection, while that of RNase had limited effect on its antibacterial property. Importantly, nucleases moieties generally did not present negative effects on L929 cell adhesion. We believe that the nuclease coating strategy that does not place a direct evolutionary pressure on the bacteria to develop resistance will present a promising approach for imparting both antibacterial infection and tissue integration to polymeric biomaterials.

ASSOCIATED CONTENT

Supporting Information

Grafting density of PCA versus UV irradiation time, N_{1s} core-level spectra, representative CLSM images of *E. coli* adhesion and biofilm formation on inactive DNase- and RNase-functionalized samples and percentage of occupied area of *E. coli* on various substrates after incubation in growth medium for 60 min and 10 h, WCA values, representative CLSM images for *S. aureus* adhesion after pretreatment with BFg protein and percentages of bacteria area of *S. aureus* on various substrata before and after pretreatment with of BFg protein. This material is available free of charge via the Internet at http://pubs.acs.org.

AUTHOR INFORMATION

Corresponding Authors

*Tel.: +86 431 85262109; fax: +86 431 85262109; e-mail: sfluan@ciac.ac.cn.

*Tel.: +86 431 85262109; fax: +86 431 85262109; e-mail: yinjh@ciac.ac.cn.

Notes

The authors declare no competing financial interest.

ACKNOWLEDGMENTS

The authors acknowledge the financial support of the National Natural Science Foundation of China (Projects 21274150, 51273200, and 51473167), Chinese Academy of Sciences-Wego Group High-tech Research & Development Program (ZKYWG2013-01), and Scientific Development Program of Jilin Province (20130102064JC).

REFERENCES

(1) Luan, S.; Zhao, J.; Yang, H.; Shi, H.; Jin, J.; Li, X.; Liu, J.; Wang, J.; Yin, J.; Stagnaro, P. Surface Modification of Poly(styrene-*b*-(ethylene-*co*-butylene)-*b*-styrene) Elastomer via UV-Induced Graft Polymerization of *N*-vinyl Pyrrolidone. *Colloids Surf., B* **2012**, *93*, 127–134.

(2) Puskas, J. E.; Chen, Y. H. Biomedical Application of Commercial Polymers and Novel Polyisobutylene-Based Thermoplastic Elastomers for Soft Tissue Replacement. *Biomacromolecules* **2004**, *5*, 1141−1154.
(3) Lim, G. T.; Puskas, J. E.; Reneker, D. H.; Jakli, A.; Horton, W. E. Highly Hydrophobic Electrospun Fiber Mats from Polyisobutylene-Based Thermoplastic Elastomers. *Biomacromolecules* **2011**, *12*, 1795−1799.
(4) Puskas, J. E.; Foreman-Orlowski, E. A.; Lim, G. T.; Porosky, S. E.; Evancho-Chapman, M. M.; Schmidt, S. P.; El Fray, M.; Piatek, M.; Prowans, P.; Lovejoy, K. A Nanostructured Carbon-Reinforced Polyisobutylene-Based Thermoplastic Elastomer. *Biomaterials* **2010**, *31*, 2477−2488.
(5) Pinchuk, L.; Wilson, G. J.; Barry, J. J.; Schoephoerster, R. T.; Parel, J. M.; Kennedy, J. P. Medical Applications of Poly(styrene-block-isobutylene-block-styrene) ("SIBS"). *Biomaterials* **2008**, *29*, 448−460.
(6) Banerjee, I.; Pangule, R. C.; Kane, R. S. Antifouling Coatings: Recent Developments in the Design of Surfaces that Prevent Fouling by Proteins, Bacteria, and Marine Organisms. *Adv. Mater.* **2011**, *23*, 690−718.
(7) Hook, A. L.; Chang, C. Y.; Yang, J.; Luckett, J.; Cockayne, A.; Atkinson, S.; Mei, Y.; Bayston, R.; Irvine, D. J.; Langer, R.; Anderson, D. G.; Williams, P.; Davies, M. C.; Alexander, M. R. Combinatorial Discovery of Polymers Resistant to Bacterial Attachment. *Nat. Biotechnol.* **2012**, *30*, 868−875.
(8) Sileika, T. S.; Kim, H. D.; Maniak, P.; Messersmith, P. B. Antibacterial Performance of Polydopamine-Modified Polymer Surfaces Containing Passive and Active Components. *ACS Appl. Mater. Interfaces* **2011**, *3*, 4602−4610.
(9) Ma, H. W.; Hyun, J. H.; Stiller, P.; Chilkoti, A. "Non-fouling" Oligo(ethylene glycol)-Functionalized Polymer Brushes Synthesized by Surface-Initiated Atom Transfer Radical Polymerization. *Adv. Mater.* **2004**, *16*, 338−341.
(10) Yang, W. J.; Cai, T.; Neoh, K. G.; Kang, E. T.; Teo, S. L. M.; Rittschof, D. Barnacle Cement as Surface Anchor for "Clicking" of Antifouling and Antimicrobial Polymer Brushes on Stainless Steel. *Biomacromolecules* **2013**, *14*, 2041−2051.
(11) Zhao, J.; Song, L. J.; Shi, Q.; Luan, S. F.; Yin, J. H. Antibacterial and Hemocompatibility Switchable Polypropylene Nonwoven Fabric Membrane Surface. *ACS Appl. Mater. Interfaces* **2013**, *5*, 5260−5268.
(12) Cheng, G.; Xite, H.; Zhang, Z.; Chen, S. F.; Jiang, S. Y. A Switchable Biocompatible Polymer Surface with Self-Sterilizing and Nonfouling Capabilities. *Angew. Chem., Int. Ed.* **2008**, *47*, 8831−8834.
(13) Cao, Z.; Mi, L.; Mendiola, J.; Ella-Menye, J. R.; Zhang, L.; Xue, H.; Jiang, S. Y. Reversibly Switching the Function of a Surface Between Attacking and Defending against Bacteria. *Angew. Chem., Int. Ed.* **2012**, *51*, 2602−2605.
(14) Ji, F. Q.; Lin, W. F.; Wang, Z.; Wang, L. G.; Zhang, J.; Ma, G. L.; Chen, S. F. Development of Nonstick and Drug-Loaded Wound Dressing Based on the Hydrolytic Hydrophobic Poly(carboxybetaine) Ester Analogue. *ACS Appl. Mater. Interfaces* **2013**, *5*, 10489−10494.
(15) Cao, B.; Tang, Q.; Li, L. L.; Humble, J.; Wu, H. Y.; Liu, L. Y.; Cheng, G. Switchable Antimicrobial and Antifouling Hydrogels with Enhanced Mechanical Properties. *Adv. Healthcare Mater.* **2013**, *2*, 1096−1102.
(16) Sin, M. C.; Sun, Y. M.; Chang, Y. Zwitterionic-Based Stainless Steel with Well-Defined Polysulfobetaine Brushes for General Bioadhesive Control. *ACS Appl. Mater. Interfaces* **2014**, *6*, 861−873.
(17) Lalani, R.; Liu, L. Y. Electrospun Zwitterionic Poly(Sulfobetaine Methacrylate) for Nonadherent, Superabsorbent, and Antimicrobial Wound Dressing Applications. *Biomacromolecules* **2012**, *13*, 1853−1863.
(18) Carr, L.; Cheng, G.; Xue, H.; Jiang, S. Y. Engineering the Polymer Backbone to Strengthen Nonfouling Sulfobetaine Hydrogels. *Langmuir* **2010**, *26*, 14793−14798.
(19) Jiang, S. Y.; Cao, Z. Q. Ultralow-Fouling, Functionalizable, and Hydrolyzable Zwitterionic Materials and Their Derivatives for Biological Applications. *Adv. Mater.* **2010**, *22*, 920−932.
(20) Chen, S. G.; Chen, S. J.; Jiang, S.; Xiong, M. L.; Luo, J. X.; Tang, J. N.; Ge, Z. C. Environmentally Friendly Antibacterial Cotton Textiles Finished with Siloxane Sulfopropylbetaine. *ACS Appl. Mater. Interfaces* **2011**, *3*, 1154−1162.
(21) Diaz Blanco, C.; Ortner, A.; Dimitrov, R.; Navarro, A.; Mendoza, E.; Tzanov, T. Building an Antifouling Zwitterionic Coating on Urinary Catheters Using an Enzymatically Triggered Bottom-Up Approach. *ACS Appl. Mater. Interfaces* **2014**, *6*, 11385−11393.
(22) Rodriguez-Emmenegger, C.; Houska, M.; Alles, A. B.; Brynda, E. Surfaces Resistant to Fouling from Biological Fluids: Towards Bioactive Surfaces for Real Applications. *Macromol. Biosci.* **2012**, *12*, 1413−1422.
(23) Liu, Q. S.; Singh, A.; Lalani, R.; Liu, L. Y. Ultralow Fouling Polyacrylamide on Gold Surfaces via Surface-Initiated Atom Transfer Radical Polymerization. *Biomacromolecules* **2012**, *13*, 1086−1092.
(24) Li, M.; Neoh, K. G.; Kang, E. T.; Lau, T.; Chiong, E. Surface Modification of Silicone with Covalently Immobilized and Crosslinked Agarose for Potential Application in the Inhibition of Infection and Omental Wrapping. *Adv. Funct Mater.* **2014**, *24*, 1631−1643.
(25) Jiang, J. H.; Zhu, L. P.; Zhu, L. J.; Zhang, H. T.; Zhu, B. K.; Xu, Y. Y. Antifouling and Antimicrobial Polymer Membranes Based on Bioinspired Polydopamine and Strong Hydrogen-Bonded Poly(*N*-vinyl pyrrolidone). *ACS Appl. Mater. Interfaces* **2013**, *5*, 12895−12904.
(26) Aumsuwan, N.; McConnell, M. S.; Urban, M. W. Tunable Antimicrobial Polypropylene Surfaces: Simultaneous Attachment of Penicillin (Gram +) and Gentamicin (Gram −). *Biomacromolecules* **2009**, *10*, 623−629.
(27) Wang, H. R.; Cheng, M.; Hu, J. M.; Wang, C. H.; Xu, S. S.; Han, C. C. Preparation and Optimization of Silver Nanoparticles Embedded Electrospun Membrane for Implant Associated Infections Prevention. *ACS Appl. Mater. Interfaces* **2013**, *5*, 11014−11021.
(28) Hui, F.; Debiemme-Chouvy, C. Antimicrobial *N*-Halamine Polymers and Coatings: A Review of Their Synthesis, Characterization, and Applications. *Biomacromolecules* **2013**, *14*, 585−601.
(29) Kocer, H. B.; Cerkez, I.; Worley, S. D.; Broughton, R. M.; Huang, T. S. *N*-Halamine Copolymers for Use in Antimicrobial Paints. *ACS Appl. Mater. Interfaces* **2011**, *3*, 3189−3194.
(30) Ding, X.; Yang, C.; Lim, T. P.; Hsu, L. Y.; Engler, A. C.; Hedrick, J. L.; Yang, Y. Y. Antibacterial and Antifouling Catheter Coatings Using Surface Grafted PEG-*b*-Cationic Polycarbonate Diblock Copolymers. *Biomaterials* **2012**, *33*, 6593−6603.
(31) Shi, Z. L.; Neoh, K. G.; Kang, E. T.; Wang, W. Antibacterial and Mechanical Properties of Bone Cement Impregnated with Chitosan Nanoparticles. *Biomaterials* **2006**, *27*, 2440−2449.
(32) Liu, L. H.; Xu, K. J.; Wang, H. Y.; Tan, P. K. J.; Fan, W. M.; Venkatraman, S. S.; Li, L. J.; Yang, Y. Y. Self-Assembled Cationic Peptide Nanoparticles as an Efficient Antimicrobial Agent. *Nat. Nanotechnol.* **2009**, *4*, 457−463.
(33) Krumm, C.; Harmuth, S.; Hijazi, M.; Neugebauer, B.; Kampmann, A. L.; Geltenpoth, H.; Sickmann, A.; Tiller, J. C. Antimicrobial Poly(2-methyloxazoline)s with Bioswitchable Activity through Satellite Group Modification. *Angew. Chem., Int. Ed.* **2014**, *53*, 3830−3834.
(34) Fernandes, M. M.; Francesko, A.; Torrent-Burgues, J.; Carrion-Fite, F. J.; Heinze, T.; Tzanov, T. Sonochemically Processed Cationic Nanocapsules: Efficient Antimicrobials with Membrane Disturbing Capacity. *Biomacromolecules* **2014**, *15*, 1365−1374.
(35) Petkova, P.; Francesko, A.; Fernandes, M. M.; Mendoza, E.; Perelshtein, I.; Gedanken, A.; Tzanov, T. Sonochemical Coating of Textiles with Hybrid ZnO/Chitosan Antimicrobial Nanoparticles. *ACS Appl. Mater. Interfaces* **2014**, *6*, 1164−1172.
(36) Dinu, C. Z.; Zhu, G.; Bale, S. S.; Anand, G.; Reeder, P. J.; Sanford, K.; Whited, G.; Kane, R. S.; Dordick, J. S. Enzyme-Based Nanoscale Composites for Use as Active Decontamination Surfaces. *Adv. Funct. Mater.* **2010**, *20*, 392−398.
(37) Loeffler, J. M.; Nelson, D.; Fischetti, V. A. Rapid Killing of *Streptococcus pneumoniae* with a Bacteriophage Cell Wall Hydrolase. *Science* **2001**, *294*, 2170−2172.

(38) Wang, Y.; Subbiahdoss, G.; Swartjes, J.; van der Mei, H. C.; Busscher, H. J.; Libera, M. Length-Scale Mediated Differential Adhesion of Mammalian Cells and Microbes. *Adv. Funct. Mater.* **2011**, *21*, 3916−3923.
(39) Wang, Y.; Domingues, J. E. D.; Subbiandoss, G.; van der Mei, H. C.; Busscher, H. J.; Libera, M. Conditions of Lateral Surface Confinement that Promote Tissue-cell Integration and Inhibit Biofilm Growth. *Biomaterials* **2014**, *35*, 5446−5452.
(40) Chua, P. H.; Neoh, K. G.; Kang, E. T.; Wang, W. Surface Functionalization of Titanium with Hyaluronic Acid/Chitosan Polyelectrolyte Multilayers and RGD for Promoting Osteoblast Functions and Inhibiting Bacterial Adhesion. *Biomaterials* **2008**, *29*, 1412−1421.
(41) Flemming, H. C.; Wingender, J. The Biofilm Matrix. *Nat. Rev. Microbiol.* **2010**, *8*, 623−633.
(42) Chambers, J. R.; Sauer, K. Small RNAs and Their Role in Biofilm Formation. *Trends Microbiol.* **2013**, *21*, 39−49.
(43) Whitchurch, C. B.; Tolker-Nielsen, T.; Ragas, P. C.; Mattick, J. S. Extracellular DNA Required for Bacterial Biofilm Formation. *Science* **2002**, *295*, 1487−1487.
(44) Ghaz-Jahanian, M. A.; Khodaparastan, F.; Berenjian, A.; Jafarizadeh-Malmiri, H. Influence of Small RNAs on Biofilm Formation Process in Bacteria. *Mol. Biotechnol.* **2013**, *55*, 288−297.
(45) Tetz, G. V.; Artemenko, N. K.; Tetz, V. V. Effect of DNase and Antibiotics on Biofilm Characteristics. *Antimicrob. Agents Chemother.* **2009**, *53*, 1204−1209.
(46) Thomas, V. C.; Thurlow, L. R.; Boyle, D.; Hancock, L. E. Regulation of Autolysis-Dependent Extracellular DNA Release by Enterococcus Faecalis Extracellular Proteases Influences Biofilm Development. *J. Bacteriol.* **2008**, *190*, 5690−5698.
(47) Swartjes, J. J. T. M.; Das, T.; Sharifi, S.; Subbiahdoss, G.; Sharma, P. K.; Krom, B. P.; Busscher, H. J.; van der Mei, H. C. A Functional DNase I Coating to Prevent Adhesion of Bacteria and the Formation of Biofilm. *Adv. Funct. Mater.* **2013**, *23*, 2843−2849.
(48) Yang, W. J.; Cai, T.; Neoh, K. G.; Kang, E. T.; Dickinson, G. H.; Teo, S. L. M.; Rittschof, D. Biomimetic Anchors for Antifouling and Antibacterial Polymer Brushes on Stainless Steel. *Langmuir* **2011**, *27*, 7065−7076.
(49) Edlund, U.; Kallrot, M.; Albertsson, A. C. Single-Step Covalent Functionalization of Polylactide Surfaces. *J. Am. Chem. Soc.* **2005**, *127*, 8865−8871.
(50) Kallrot, M.; Edlund, U.; Albertsson, A. C. Surface Functionalization of Degradable Polymers by Covalent Grafting. *Biomaterials* **2006**, *27*, 1788−1796.
(51) Tang, S. C.; Xie, J. Y.; Huang, Z. H.; Xu, F. J.; Yang, W. T. UV-Induced Grafting Processes with In Situ Formed Photomask for Micropatterning of Two-Component Biomolecules. *Langmuir* **2010**, *26*, 9905−9910.
(52) Kallrot, M.; Edlund, U.; Albertsson, A. C. Surface Functionalization of Porous Resorbable Scaffolds by Covalent Grafting. *Macromol. Biosci.* **2008**, *8*, 645−654.
(53) Mahmoud, K. A.; Male, K. B.; Hrapovic, S.; Luong, J. H. T. Cellulose Nanocrystal/Gold Nanoparticle Composite as a Matrix for Enzyme Immobilization. *ACS Appl. Mater. Interfaces* **2009**, *1*, 1383−1386.
(54) Busscher, H. J.; van der Mei, H. C.; Subbiahdoss, G.; Jutte, P. C.; van den Dungen, J. J. A. M.; Zaat, S. A. J.; Schultz, M. J.; Grainger, D. W. Biomaterial-Associated Infection: Locating the Finish Line in the Race for the Surface. *Sci. Transl. Med.* **2012**, *4*, 153rv10.
(55) Tuson, H. H.; Weibel, D. B. Bacteria-Surface Interactions. *Soft Matter* **2013**, *9*, 4368−4380.
(56) Rosenberg, H. F. Recombinant Human Eosinophil Cationic Protein-Ribonuclease-Activity Is Not Essential for Cytotoxicity. *J. Biol. Chem.* **1995**, *270*, 7876−7881.
(57) Carreras, E.; Boix, E.; Rosenberg, H. F.; Cuchillo, C. M.; Nogues, M. V. Both Aromatic and Cationic Residues Contribute to the Membrane-Lytic and Bactericidal Activity of Eosinophil Cationic Protein. *Biochemistry* **2003**, *42*, 6636−6644.
(58) Poelstra, K. A.; Barekzi, N. A.; Rediske, A. M.; Felts, A. G.; Slunt, J. B.; Grainger, D. W. Prophylactic Treatment of Gram-Positive and Gram-Negative Abdominal Implant Infections Using Locally Delivered Polyclonal Antibodies. *J. Biomed. Mater. Res.* **2002**, *60*, 206−215.
(59) Boix, E.; Nogues, M. V. Mammalian Antimicrobial Proteins and Peptides: Overview on the RNase A Superfamily Members Involved in Innate Host Defence. *Mol. Biosyst.* **2007**, *3*, 317−335.
(60) Tedjo, C.; Neoh, K. G.; Kang, E. T.; Fang, N.; Chan, V. Bacteria-Surface Interaction in the Presence of Proteins and Surface Attached Poly(ethylene glycol) Methacrylate Chains. *J. Biomed. Mater. Res., Part A* **2007**, *82*, 479−491.
(61) Wolz, C.; McDevitt, D.; Poster, T. J.; Cheung, A. L. Influence of Agr on Fibrinogen Binding in *Staphylococcus aureus* Newman. *Infect. Immun.* **1996**, *64*, 3142−3147.